JOURNAL OF PROPULSION AND POWER
Vol. 18, No. 2, March–April 2002

Characteristic Analysis of Flow-Induced Vibrations on Inducer of Oxygen Pump

Liang Hengli* and Chen Zuoyi†
Tsinghua University, 100084 Beijing, People's Republic of China

Characteristics of flow-induced vibrations in liquid-rocket-engine oxygen turbopump inducers are analyzed because the inducers were damaged in a test. Oscillating fluid mechanics theory and parametric polynomial method are used to solve the three-dimensional, steady and unsteady basic equations. It is found that the damage was caused by the oscillating pressure propagation, where a small external perturbation from the outlet of the inducer can be transformed to a very large oscillating pressure at some low frequencies. Some characteristics of inducers are analyzed to improve the severe flow-induced vibration, such as increasing the inlet section length or the pitch, which can all decrease the pressure amplitudes effectively.

Nomenclature

a = coefficient of parametric polynomial method for W_r
b = coefficient of parametric polynomial method for W_θ
c = coefficient of parametric polynomial method for W_z
d = coefficient of parametric polynomial method for P
e = coefficient of parametric polynomial method for $\bar{W}_r$
f = coefficient of parametric polynomial method for $\bar{W}_\theta$
fr = frequency of perturbation
g = coefficient of parametric polynomial method for $\bar{W}_z$
h = coefficient of parametric polynomial method for $\bar{P}$
i = imaginary unit
P = pressure
q = any parameter of flowfield
W_r = velocity component in the r direction
W_z = velocity component in the z direction
W_θ = velocity component in the θ direction
μ = coefficient of turbulent viscosity
ρ = density
Ω = angular velocity of the inducer
ω = angular velocity of the perturbation

Subscript

0 = upstream of the inducer

Superscripts

$\sim$ = steady component
- = oscillating component

Introduction

WITHIN a liquid-rocket-engine, inducers are widely used to improve cavitation of the turbopump, which make it operate steadily under the condition of high state speed and low inlet pressure.[1] However, during operation inducers will be subject to oscillating pressure load, which is induced by oscillation, cavitation, upstream shock, or other pressure-wave vibration source of the pump system. When the flow condition is beyond a certain range, pressure and flow vibrations will occur in most inducers. The vibrations are in a low-frequency range from 5 to 40 Hz, which is the direct result of hydrodynamic couple of the inducer and parts of flow systems. They can weaken performance of the inducer in a delivery system. So far, many attentions have been paid to inducer instabilities, especially to the effects of rotating cavitation.[2–10]

Last year, in a running test of liquid-rocket-engine, the inducer of a liquid-oxygen turbopump was damaged. The posted-test analysis of the inducer showed no pitting corrosion causing by cavitation on the surface, but the inlet blades were fractured obliquely. Therefore, it should not be destroyed by cavitation. Figures 1 and 2 illustrate the seriously damaged inducers from the test. The sample in Fig. 1 was made of aluminum alloy and is the same size as the one in Fig. 2, which was made of alloyed steel. When the inducer made of aluminum alloy was damaged, the researchers conjectured that it was not strong enough for the condition. They chose the alloyed steel inducer with much greater strength than the aluminum alloy. However, it was destroyed immediately at the same flow conditions too. Analysis of the inducer showed that the inducer damage was caused by low-cycle fatigue caused by tremendous pressure vibrations. Therefore, the main objective of this paper is to analyze the characteristic of the flow-induced vibrations in the inducer to find out the real cause of the accident.

Four oxygen turbopump inducers were analyzed to study the effects of the flow-induced vibrations. The characteristics of the four inducers are shown in Table 1.

Water was used instead of liquid oxygen in the test as the fluid. The rotation speed of inducer was 13,000 n/min, the design volume flow rate was 0.0613 m^3/s, and the inlet pressure of the inducer was 0.29 MPa. The flow-induced vibrations were analyzed for external perturbations ranging from 20 to 1000 Hz and flow rates for 0.8, 0.9, 1.0, 1.1, and 1.2 of the design flow rate.

Mathematical Method

Flow-induced vibrations of a liquid-oxygen turbopump inducer are related to the propagation of external perturbations within the inducer. The propagation of the oscillations is an unsteady, three-dimensional viscous flow phenomenon. However, analysis of all kinds of geometries, frequencies, and flow rates would require a large number of calculations. For example, to analyze four types of inducers with five perturbation frequencies and five flow rates would need 100 analyses. If some of the geometries were changed to observe their effects on the flow, then hundreds of analyses would be needed. Therefore, it is impractical to solve the problem with conventional three-dimensional, unsteady viscous flow numerical methods. In this paper the oscillating fluid mechanics method[11] and the parametric polynomial method[12] are applied to solve the problem quickly. The oscillating fluid mechanics theory transforms the three-dimensional viscous flow equations into amplitude equations, which are solved using the parametric polynomial method.

Received 19 August 2000; revision received 23 April 2001; accepted for publication 19 September 2001. Copyright © 2001 by the American Institute of Aeronautics and Astronautics, Inc. All rights reserved. Copies of this paper may be made for personal or internal use, on condition that the copier pay the $10.00 per-copy fee to the Copyright Clearance Center, Inc., 222 Rosewood Drive, Danvers, MA 01923; include the code 0748-4658/02 $10.00 in correspondence with the CCC.

*(**Job title**), Department of Thermal Engineering.
†(**Job title**), Department of Thermal Engineering; Chenzy@te.tsinghua.edu.cn.

Table 1 Characteristics of inducers

Serial number	Blade number	Hub inlet diameter, mm	Hub outlet diameter, mm	Tip diameter, mm	Shaft length, mm	Blade thickness, mm	Blade lead
0-04	3	32	76	120	63	1.2	0 ~ 146.8 deg is 49.6 mm; 146.8 ~ 318.1 deg is variable; 318.1 ~ 374.4 deg is 70 mm
0-04J	3	42	76	120	63	1.2	0 ~ 146.8 deg is 49.6 mm; 146.8 ~ 318.1 deg is variable; 318.1 ~ 374.4 deg is 70 mm
0-04J2	3	42	76	120	63	1.2	60 mm
0-04J3	3	42	76	120	63	1.2	70 mm

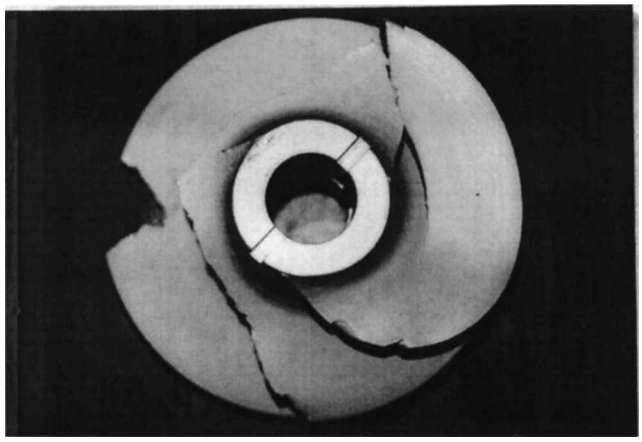

Fig. 1 Aluminum alloy sample.

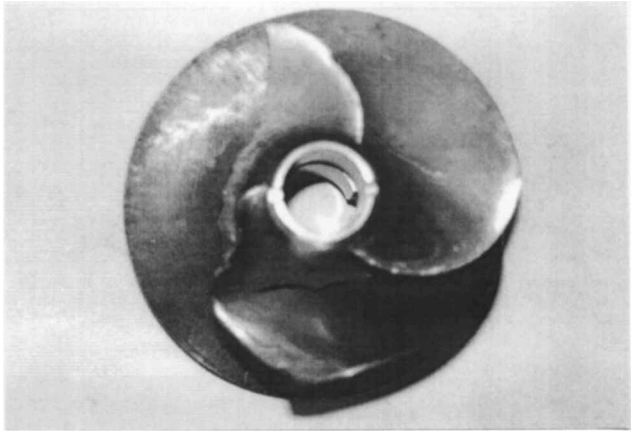

Fig. 2 Alloyed steel sample.

According to the oscillating fluid mechanics theory, a complex oscillation is superposed by simple harmonic oscillations. An unsteady flow is composed of steady flow and oscillating flow. If a very small perturbation is considered to cause the oscillating flow, then the flow parameters can be represented as

$$q(t, r, \theta, z) = \tilde{q}(r, \theta, z) + \bar{q}(r, \theta, z)e^{i\omega t} \tag{1}$$

Parameter $\tilde{q}$ designates steady component, and $\bar{q}$ designates the amplitude of oscillating component. Therefore, the governing equations can be decomposed to steady equations and oscillating equations, which can be solved sequentially.[13]

Fundamental equations for a liquid-oxygen turbopump inducer use turbine circular cylindrical coordinates. Because the fluid through the inducer is liquid, the flow is considered to be incompressible.

In a three-dimensional viscous flow the basic steady-state equations are [14] as follows:

Continuity equation:

$$\rho\frac{\partial W_\theta}{r\partial\theta} = -\left(\rho\frac{W_r}{r} + \rho\frac{\partial W_r}{\partial r} + \rho\frac{\partial W_z}{\partial z}\right) \tag{2}$$

Radial momentum equation:

$$\rho W_\theta\frac{\partial W_r}{r\partial\theta} - \frac{\mu}{3}\frac{\partial^2 W_\theta}{r^2\partial\theta^2} - \mu\frac{\partial^2 W_r}{r^2\partial\theta^2} + \mu\frac{7}{3}\frac{\partial W_\theta}{r^2\partial\theta} = -\frac{\partial P}{\partial r} - \rho\left(W_r\frac{\partial W_r}{\partial r} + W_z\frac{\partial W_r}{\partial z} - \frac{W_\theta^2}{r} - 2W_\theta\Omega - r\Omega^2\right) + \mu\left(\frac{4}{3}\frac{\partial^2 W_r}{\partial r^2} + \frac{1}{3}\frac{\partial^2 W_z}{\partial r\partial z} + \frac{\partial^2 W_r}{\partial z^2} + \frac{4}{3}\frac{\partial W_r}{r\partial r} - \frac{4}{3}\frac{W_r}{r^2}\right) \tag{3}$$

Circumferential momentum equation:

$$\frac{\partial P}{r\partial\theta} + \rho W_\theta\frac{\partial W_\theta}{r\partial\theta} - \mu\left(\frac{4}{3}\frac{\partial^2 W_\theta}{r^2\partial\theta^2} + \frac{1}{3}\frac{\partial^2 W_z}{r\partial z\partial\theta} - \frac{1}{3}\frac{\partial^2 W_r}{r\partial r\partial\theta} - \frac{7}{3}\frac{\partial W_r}{r^2\partial\theta}\right) = -\rho\left(W_r\frac{\partial W_\theta}{\partial r} + W_z\frac{\partial W_\theta}{\partial z} + \frac{W_r W_\theta}{r} + 2\Omega W_r\right) + \mu\left(\frac{\partial^2 W_\theta}{\partial r^2} + \frac{\partial^2 W_\theta}{\partial z^2} - \frac{W_\theta}{r^2} + \frac{\partial W_\theta}{r\partial r}\right) \tag{4}$$

Axial momentum equation:

$$\rho W_\theta\frac{\partial W_z}{r\partial\theta} - \mu\left(\frac{1}{3}\frac{\partial^2 W_\theta}{r\partial z\partial\theta} + \frac{\partial^2 W_z}{r^2\partial\theta^2}\right) = -\frac{\partial P}{\partial z} - \rho\left(W_r\frac{\partial W_z}{\partial r} + W_z\frac{\partial W_z}{\partial z}\right) + \mu\left(\frac{\partial^2 W_z}{\partial r^2} + \frac{\partial W_z}{r\partial r} + \frac{1}{3}\frac{\partial^2 W_r}{\partial z\partial r} + \frac{4}{3}\frac{\partial^2 W_z}{\partial z^2} + \frac{1}{3}\frac{\partial W_r}{r\partial z}\right) \tag{5}$$

Wall boundary conditions:

$$W_r = 0, \qquad W_\theta = 0, \qquad W_z = 0 \tag{6}$$

Inlet boundary conditions:

$$W_r = W_{r0}, \qquad W_\theta = W_{\theta 0}, \qquad W_z = W_{z0} \tag{7}$$

The steady-state parameters can be represented in parametric polynomial form:

$$W_r = \sum_{j=0}^{J}\sum_{k=0}^{K} a_{jk} r^j z^k \tag{8}$$

$$W_\theta = \sum_{j=0}^{J}\sum_{k=0}^{K} b_{jk} r^j z^k \tag{9}$$

$$W_z = \sum_{j=0}^{J}\sum_{k=0}^{K} c_{jk} r^j z^k \tag{10}$$

$$P = \sum_{j=0}^{J}\sum_{k=0}^{K} d_{jk} r^j z^k \tag{11}$$

where $J = 3$ and $K = 3$.

The flow is calculated along circumference, which is divided equally to 300 computer stations. For each state, a_{jk}, b_{jk}, c_{jk}, and d_{jk}, which are independent of r and z, have their corresponding values by solving the preceding equations.

Similarly, in a three-dimensional viscous flow the basic oscillating equations are as follows:

Continuity equation:

$$\tilde{\rho}\frac{\partial \bar{W}_\theta}{r\partial\theta} = -\left(\tilde{\rho}\frac{\partial \bar{W}_r}{\partial r} + \bar{W}_r\frac{\tilde{\rho}}{r} + \tilde{\rho}\frac{\partial \bar{W}_z}{\partial z}\right) \tag{12}$$

Radial momentum equation:

$$\begin{aligned}\tilde{\rho}\left(i\omega\bar{W}_r + \tilde{W}_\theta\frac{\partial \bar{W}_r}{r\partial\theta}\right) - \frac{\mu}{3r^2}\left(3\frac{\partial^2 \bar{W}_r}{\partial\theta^2} + \frac{\partial^2 \bar{W}_\theta}{\partial\theta^2} - 7\frac{\partial \bar{W}_\theta}{\partial\theta}\right)\\ = -\frac{\partial \bar{P}}{\partial r} - \tilde{\rho}\left(\tilde{W}_r\frac{\partial \bar{W}_r}{\partial r} + \bar{W}_r\frac{\partial \tilde{W}_r}{\partial r} + \bar{W}_z\frac{\partial \tilde{W}_r}{\partial z}\right.\\ \left. + \tilde{W}_z\frac{\partial \bar{W}_r}{\partial z} - 2\frac{\bar{W}_\theta\tilde{W}_\theta}{r} - 2\bar{W}_\theta\Omega\right) + \frac{\mu}{3}\left(4\frac{\partial^2 \bar{W}_r}{\partial r^2} + 4\frac{\partial \bar{W}_r}{r\partial r}\right.\\ \left. - 4\frac{\bar{W}_r}{r^2} + \frac{\partial^2 \bar{W}_z}{\partial z\partial r} + 3\frac{\partial^2 \bar{W}_r}{\partial z^2}\right)\end{aligned} \tag{13}$$

Circumferential momentum equation:

$$\begin{aligned}\tilde{\rho}i\omega\bar{W}_\theta + \frac{\partial \bar{P}}{r\partial\theta} + \tilde{\rho}\tilde{W}_\theta\frac{\partial \bar{W}_\theta}{r\partial\theta} - \frac{\mu}{3r}\left(4\frac{\partial^2 \bar{W}_\theta}{r\partial\theta^2} + \frac{\partial^2 \bar{W}_z}{\partial z\partial\theta} - \frac{\partial^2 \bar{W}_r}{\partial r\partial\theta}\right.\\ \left. - 7\frac{\partial \bar{W}_r}{r\partial\theta}\right) = -\tilde{\rho}\left(\frac{\bar{W}_r\tilde{W}_\theta}{r} + \frac{\tilde{W}_r\bar{W}_\theta}{r} + \bar{W}_z\frac{\partial \tilde{W}_\theta}{\partial z} + \tilde{W}_z\frac{\partial \bar{W}_\theta}{\partial z}\right.\\ \left. + \bar{W}_r\frac{\partial \tilde{W}_\theta}{\partial r} + \tilde{W}_r\frac{\partial \bar{W}_\theta}{\partial r}\right) - \tilde{\rho}\left(\bar{W}_\theta\frac{\partial \tilde{W}_\theta}{r\partial\theta} + 2\Omega\bar{W}_r\right)\\ + \mu\left(\frac{\partial^2 \bar{W}_\theta}{\partial r^2} + \frac{\partial^2 \bar{W}_\theta}{\partial z^2} - \frac{\bar{W}_\theta}{r^2} + \frac{\partial \bar{W}_\theta}{r\partial r}\right)\end{aligned} \tag{14}$$

Axial momentum equation:

$$\begin{aligned}\tilde{\rho}\left(\bar{W}_z i\omega + \tilde{W}_\theta\frac{\partial \bar{W}_z}{r\partial\theta}\right) - \frac{\mu}{3r}\left(\frac{\partial^2 \bar{W}_\theta}{\partial z\partial\theta} + \frac{3}{r}\frac{\partial^2 \bar{W}_z}{\partial\theta^2}\right) = -\frac{\partial \bar{P}}{\partial z}\\ - \tilde{\rho}\left(\bar{W}_\theta\frac{\partial \tilde{W}_z}{r\partial\theta} + \bar{W}_r\frac{\partial \tilde{W}_z}{\partial r} + \tilde{W}_r\frac{\partial \bar{W}_z}{\partial r} + \bar{W}_z\frac{\partial \tilde{W}_z}{\partial z} + \tilde{W}_z\frac{\partial \bar{W}_z}{\partial z}\right)\\ + \frac{\mu}{3}\left(\frac{\partial^2 \bar{W}_r}{\partial z\partial r} + 4\frac{\partial^2 \bar{W}_z}{\partial z^2} + \frac{\partial \bar{W}_r}{r\partial z} + 3\frac{\partial^2 \bar{W}_z}{\partial r^2} + 3\frac{\partial \bar{W}_z}{r\partial r}\right)\end{aligned} \tag{15}$$

The amplitude parameters can be represented in parametric polynomial form:

$$\bar{W}_r = \sum_{j=0}^{J}\sum_{k=0}^{K} e_{jk} r^j z^k \tag{16}$$

$$\bar{W}_\theta = \sum_{j=0}^{J}\sum_{k=0}^{K} f_{jk} r^j z^k \tag{17}$$

$$\bar{W}_z = \sum_{j=0}^{J}\sum_{k=0}^{K} g_{jk} r^j z^k \tag{18}$$

$$\bar{P} = \sum_{j=0}^{J}\sum_{k=0}^{K} h_{jk} r^j z^k \tag{19}$$

where $J = 2$ and $k = 2$. They are then substituted into the oscillating governing equations to be solved for the oscillating flowfield.

Results and Discussions

Calculations were performed for external perturbations from 5 to 1000 Hz. Here we present results for 20 and 60 Hz because they provide a representative sampling of the effect of perturbation frequencies. Figures 3 and 4 show the pressure amplitude distributions along circumference for four inducers, which are induced by outlet external perturbation at 20 Hz. Figures 5 and 6 show the pressure amplitude distributions induced by inlet external perturbation at 20 Hz.

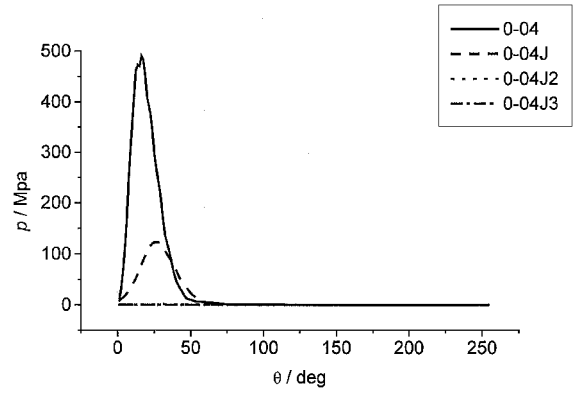

Fig. 3 Pressure distributions of outlet perturbation (*fr* = 20 Hz).

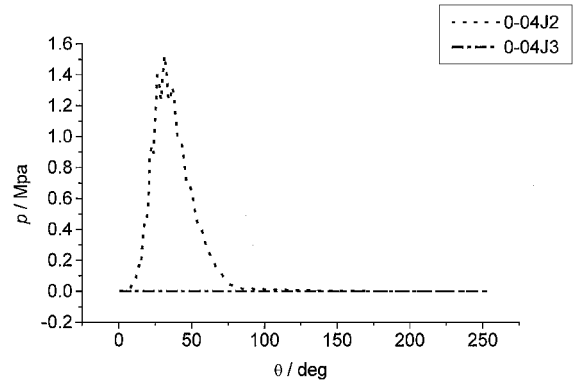

Fig. 4 Pressure distributions of outlet perturbation (*fr* = 20 Hz).

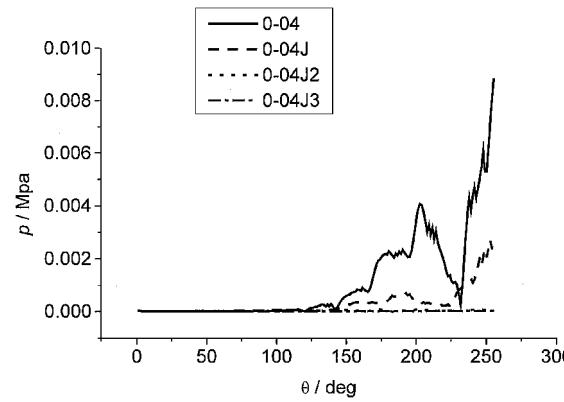

Fig. 5 Pressure distributions of inlet perturbation (*fr* = 20 Hz).

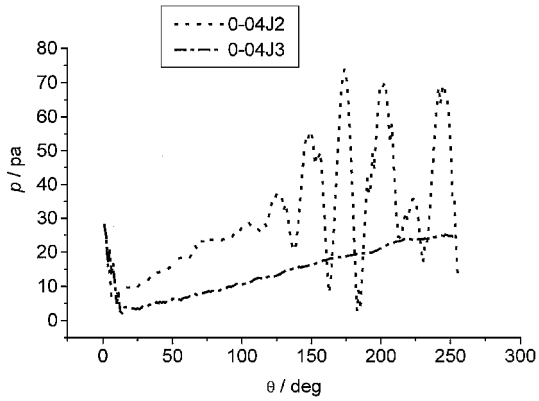

Fig. 6 Pressure distributions of inlet perturbation (*fr* = 20 Hz).

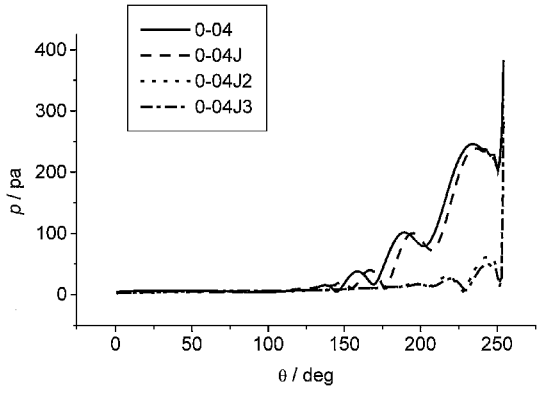

Fig. 7 Pressure distributions of outlet perturbation (*fr* = 60 Hz).

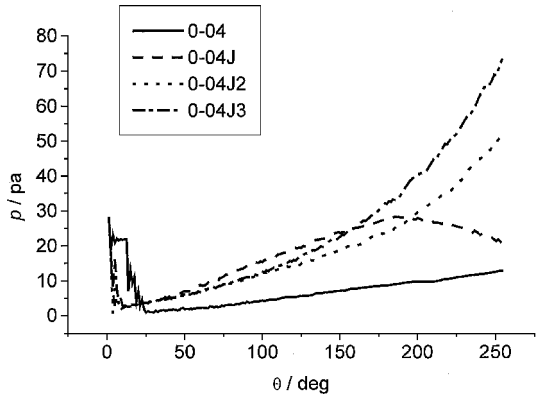

Fig. 8 Pressure distributions of inlet perturbation (*fr* = 60 Hz).

From these figures we can see that vibrations in 0-04 are the largest, then 0-04J, and vibrations in 0-04J3 are the smallest. There is a very large pressure amplitude in the inlet section of the inducers. Actually, the fracture accident occurred just at that section. Comparison of Figs. 3 and 5 also shows that the effect of inlet external perturbations is much slighter than the outlet perturbations. Figure 7 shows that the oscillations induced by outlet external perturbations at 60 Hz are decaying. Analyses of other perturbation frequencies show that when the perturbation frequency is more than 60 Hz it is always a decaying process. Although the oscillations in Fig. 8 are increasing, it is much lower than that of 20 Hz. Because we want to know how the liquid-oxygen turbopump inducers were damaged, we will analyze mainly the effect of outlet external perturbation at 20 Hz.

In the running test, when the relative flow rate was increased from 0.8 to 1.1, 0-04J was fractured suddenly, which was proved in our calculation results. Figures 9–12 show the similar distributions of

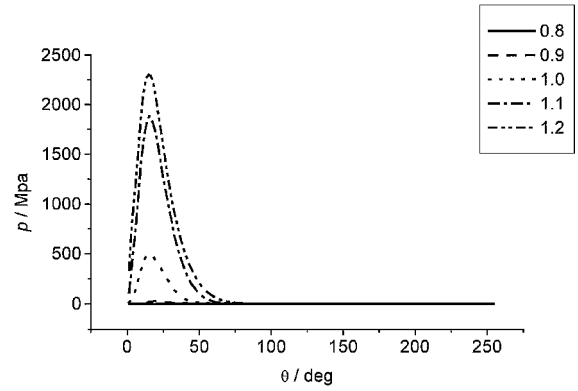

Fig. 9 Pressure distributions with different flow rate (0-04, 20 Hz, outlet).

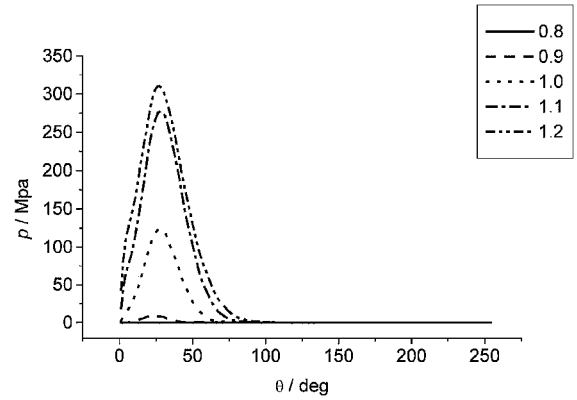

Fig. 10 Pressure distributions with different flow rate (0-04J, 20 Hz, outlet).

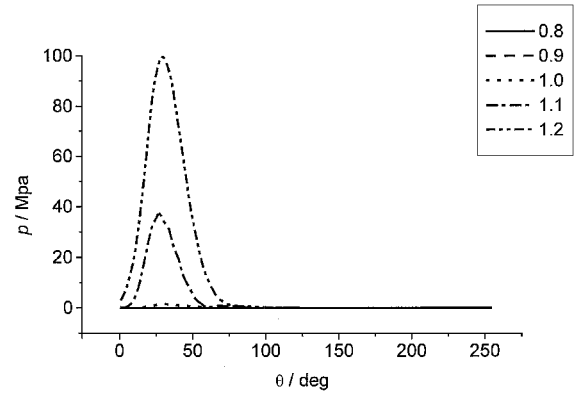

Fig. 11 Pressure distributions with different flow rate (0-04J2, 20 Hz, outlet).

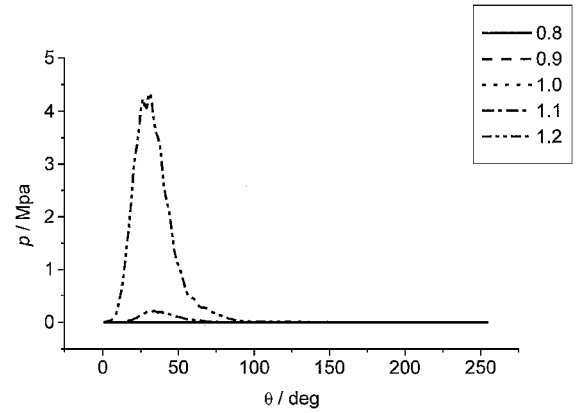

Fig. 12 Pressure distributions with different flow rate (0-04J3, 20 Hz, outlet).

oscillating pressure amplitude, which are increased with the flow rate.

Figures 3 and 5 show that a larger hub inlet diameter is helpful to reduce the vibrations, where the flow passage of 0-04J is more gentle than 0-04. Figures 4 and 6 show that a larger pitch is also helpful to reduce the vibrations, where the flow passage of 0-04J3 is also more gentle than 0-04J2. Therefore, we have an idea that a gentle flow passage should be important to improve the flow-induced vibrations of inducers. Because great vibrations occur at the inlet section of inducer, we did a test to relax the change of the inlet section. Three kinds of circumferential length are shown in Fig. 13. From Figs. 14–17 we can see that flow-induced vibrations

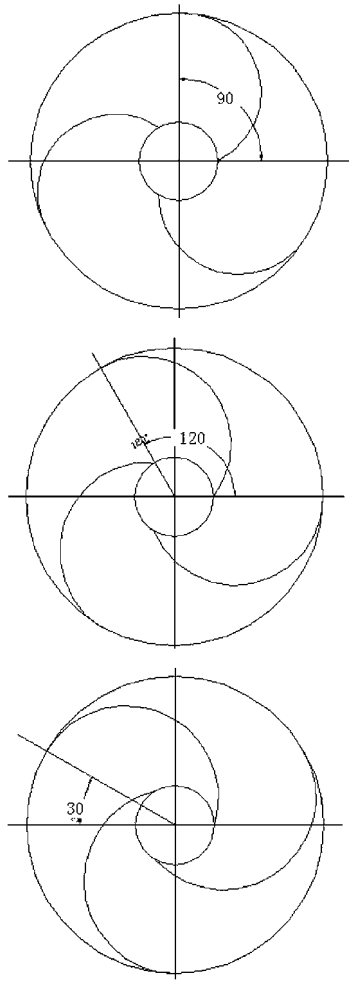

Fig. 13 Three kinds of circumferential length of inlet section (90, 120, 150 deg).

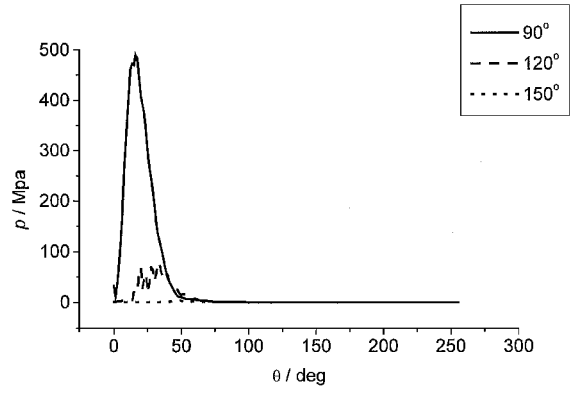

Fig. 14 Pressure distributions with different inlet length (0-04, 20 Hz, outlet).

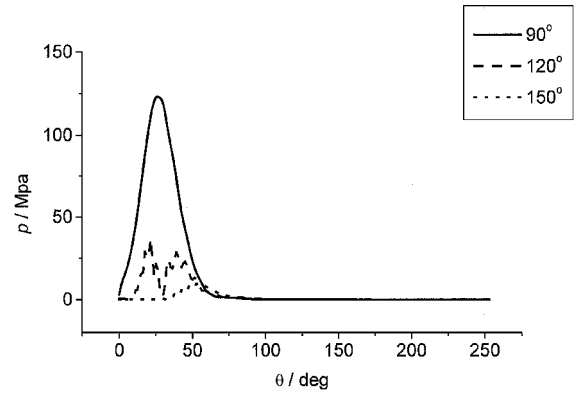

Fig. 15 Pressure distributions with different inlet length (0-04J, 20 Hz, outlet).

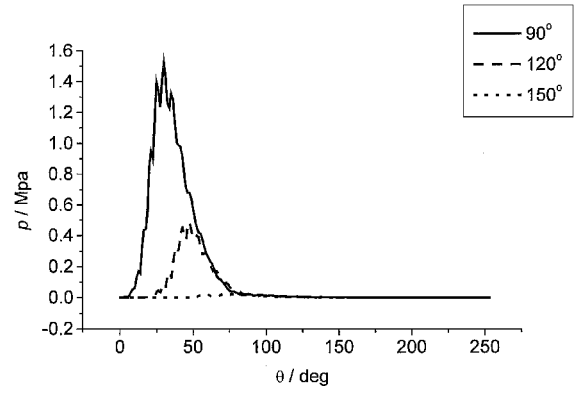

Fig. 16 Pressure distributions with different inlet length (0-04J2, 20 Hz, outlet).

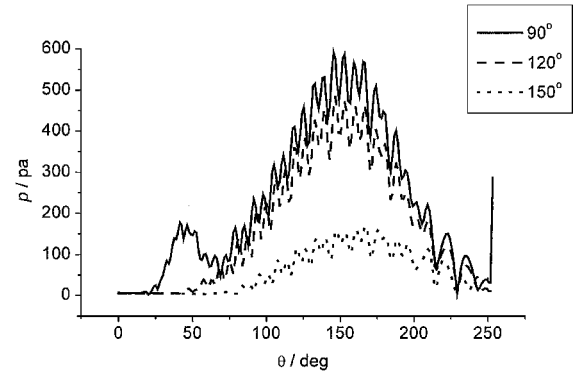

Fig. 17 Pressure distributions with different inlet length (0-04J3, 20 Hz, outlet).

are greatly decreased for all of the inducers. The design change has been used in later running tests, which effectively increased the service life of inducers.

However, we only analyze the flow-induced vibration characteristics of an inducer. The results should also be considered together with cavitation and other factors, which would also affect the flow within inducers. Our method can calculate the flow with very fast speed, but it cannot compute the precise value of each parameter. Therefore, it is better in unveiling a tendency or characteristic. Also we can say it a qualitative analysis.

Conclusions

The flow-induced vibration characteristics of liquid-oxygen turbopump inducers were analyzed using the oscillating fluid mechanics theory and the parametric polynomial method. Oscillating frequencies of external perturbation, relative flow rates, and geometries

of inducer were discussed for their effect on the vibrations of inducers. The main results that emerge from the present study led to the following conclusions:

1) The liquid-oxygen turbopump inducer damage is caused entirely by severe flow oscillations induced by the outlet external low frequency perturbations, which will generate large flow-induced pressure oscillations at the inlet section.

2) Vibrations induced by external high-frequency perturbations will be decaying in the inducer.

3) Vibrations induced by the outlet external perturbations are much larger than those induced by the inlet external perturbations.

4) Pressure oscillations are increased along with the flow rate increasing.

5) Gentle flow passage is helpful to reduce the flow-induced vibrations in the inducers, such as grade reduction, pitch increment, inlet section extension, and so on.

Acknowledgments

The research is supported by Development Plan Project of State Key Basic G1999022304. The author is also very grateful to Beijing Liquid Propulsor Research Institute for the kind help and financial aid.

References

[1]Jakbsen, J. K., "Liquid Rocket Engine Turbopump Inducers," NASA, 1971, pp. 56–69.

[2]Satoshi, W., Kazuhiko, Y., and Yoshinobu, T., "Three-Dimensional Linear Analysis of Rotating Cavitation in Inducers Using an Annular Cascade Model," *Journal of Fluids Engineering*, Vol. 121, Dec. 1999, pp. 866–871.

[3]Kamijo, K., Shimura, T., and Watanabe, M., "An Experimental Investigation of Cavitating Inducer Instability," American Society of Mechanical Engineers, Paper 77-WA/FW-14, Nov.–Dec. 1977.

[4]Kamijo, K., Yoshida, M., and Tsujimoto, Y., "Hydraulic and Mechanical Performance of LE-7 LOX Pump Induce," *Journal of Propulsion and Power*, Vol. 9, No. 6, 1993, pp. 819–826.

[5]Tsujimoto, Y., Kamijo, K., and Yoshida, Y., "A Theoretical Analysis of Rotating Cavitation in Inducers," *Journal of Fluids Engineering*, Vol. 115, No. 1, 1993, pp. 135–141.

[6]Hashimoto, T., Yoshida, M., and Watanabe, M., "Experimental Study on Rotating Cavitation of Rocket Propellant Pump Inducers," *Journal of Propulsion and Power*, Vol. 13, No. 4, 1997, pp. 488–494.

[7]Tsujimoto, Y., Yoshida, Y., and Maekawa, Y., "Observations of Oscillating Cavitation of an Inducer," *Journal of Fluids Engineering*, Vol. 119, No. 4, 1997, pp. 775–781.

[8]Otsuka, S., Tsujimoto, Y., and Kamijo, K., "Frequency Dependence of Mass Flow Gain Factor and Cavitation Compliance of Cavitating Inducers," American Society of Mechanical Engineers, Fluids Engineering Div., Vol. 190, Pt. 12 (of 18), June 1994.

[9]Stutz, B., and Reboud, J., "Experimental Study of the Two-Phase Structure of Attached Cavitation," American Society of Mechanical Engineers, Fluids Engineering Div., Vol. 194, Pt. 16 (of 18), June 1994.

[10]Maekawa, Y., Yoshida, Y., and Tsujimoto, Y., "Unsteady Interblade Pressure Distributions and Fluid Forces Under Rotating Cavitation," *Nippon Kikai Gakkai Ronbunshu*, Part B, Vol. 63, No. 605, Jan. 1997, pp. 132–138.

[11]Zuoyi, C., *Oscillating Fluid Mechanics*, Hydroelectric Press, Beijing, 1988, pp. 1–45.

[12]Zuoyi, C., *The Flow Induced Vibration*, Tsinghua Univ. Press, Beijing, 1998, pp. 28–53.

[13]Zuoyi, C., Jihong, W., and Hong, L., "Three-Dimensional Numerical Analysis of Flow-Induced Vibration in Turbomachinery," *Journal of Fluids Engineering*, Vol. 121, Dec. 1999, pp. 804–807.

[14]Xiaofeng, W., "The Three-Dimensional Aerodynamic Force and Dynamic Stress of the Vibrating Blade in Turbomachine," Ph.D. Dissertation, Dept. of Thermal Engineering, Tsinghua Univ., Beijing, June 1998, Chap. 2.